Supporting Information

Porous Organic Polymer derived carbon composite as a Bimodal Catalyst for Oxygen Evolution Reaction and Nitrophenol Reduction

Sivalingam Gopi,[a] Krishnan Giribabu[b] and Murugavel Kathiresan[a]*

[a] Electro Organic Division, CSIR-Central Electrochemical Research Institute, Karaikudi-630003, TamilNadu, INDIA. E-mail: kathiresan@cecri.res.in

[b] Electrodics and Electro Catalysis Division, CSIR-Central Electrochemical Research Institute, Karaikudi – 630003, TamilNadu, INDIA.

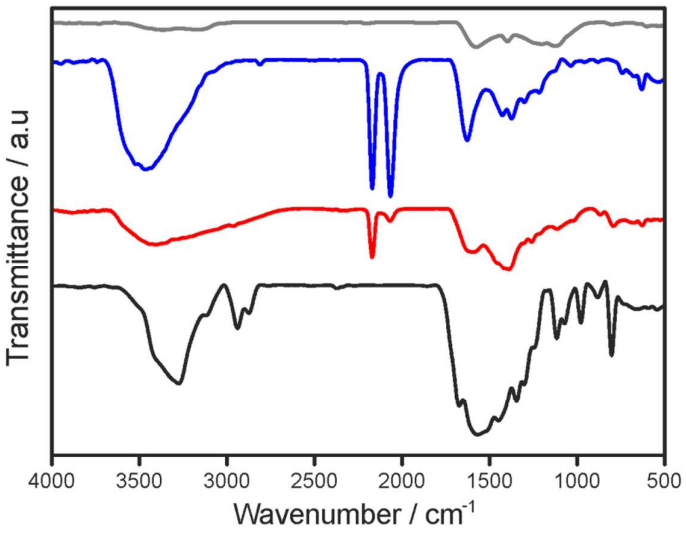

Figure S1. FT-IR spectrum of **EPOP** (black), **EPOP-600** (red), **EPOP-700** (blue) and **EPOP-800** (grey).

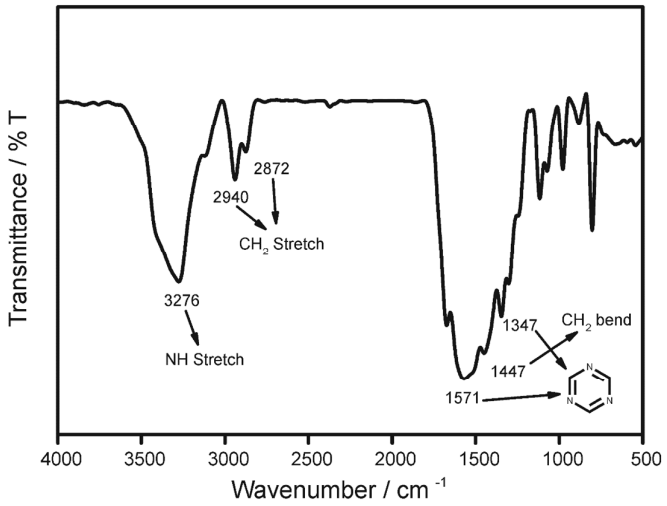

Figure S2. FT-IR spectrum of **EPOP** displaying stretching and bending frequencies of key functionalities.

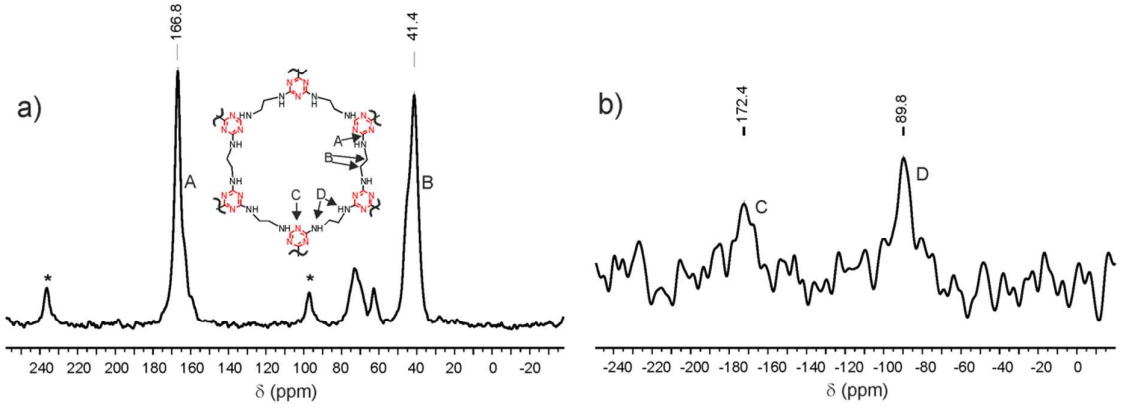

Figure S3. a) ^{13}C CP-MAS solid state NMR and b)^{15}N CP-MAS solid state NMR of **EPOP**, *denotes side bands

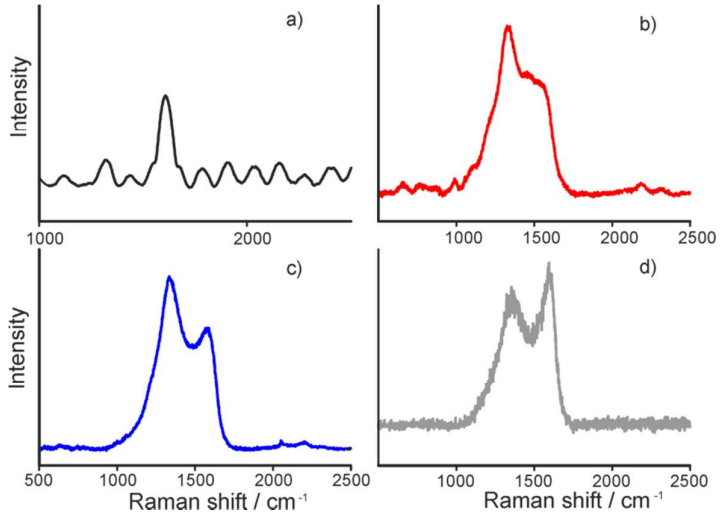

Figure S4. Raman spectra of a) **EPOP**, b) **EPOP-600**, c) **EPOP-700** and d) **EPOP-800**

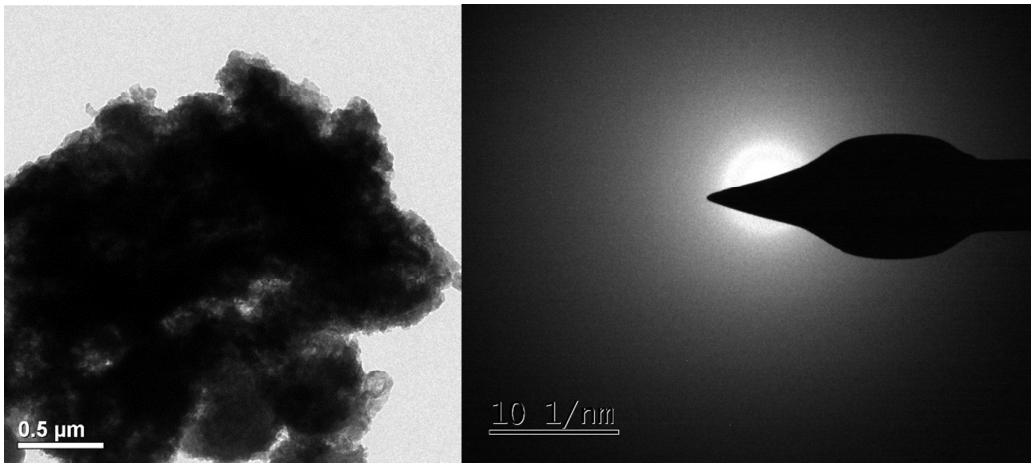

Figure S5. HR-TEM image and SAED pattern of **EPOP**

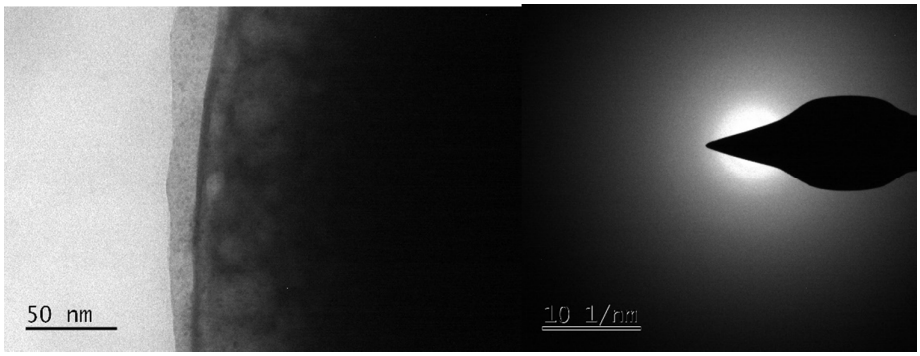

Figure S6. HR-TEM image and SAED pattern of **EPOP-600**

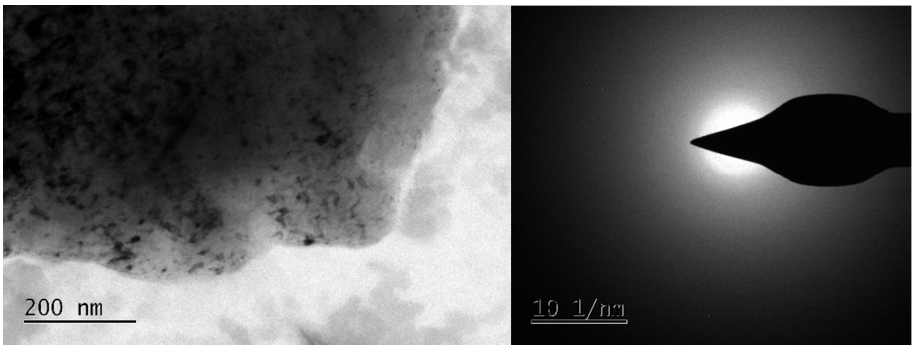

Figure S7. HR-TEM image and SAED pattern of **EPOP-700**

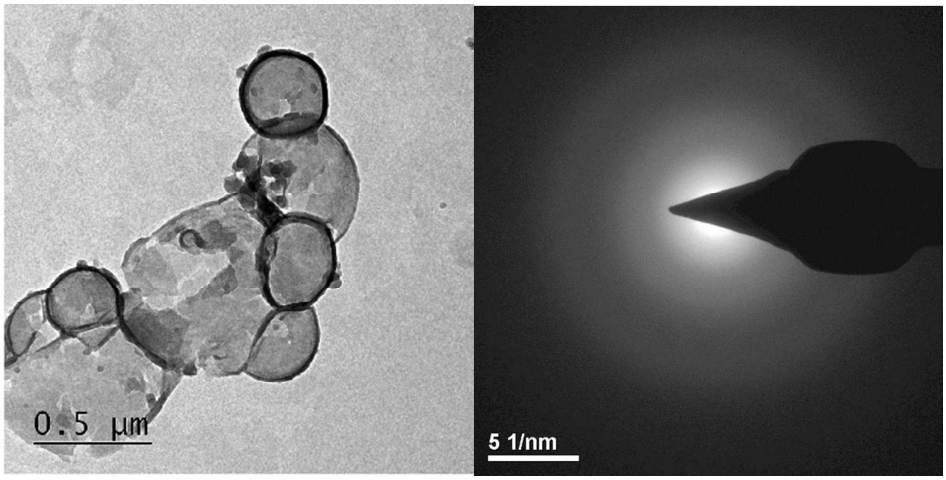

Figure S8. HR-TEM image and SAED pattern of **EPOP-800**

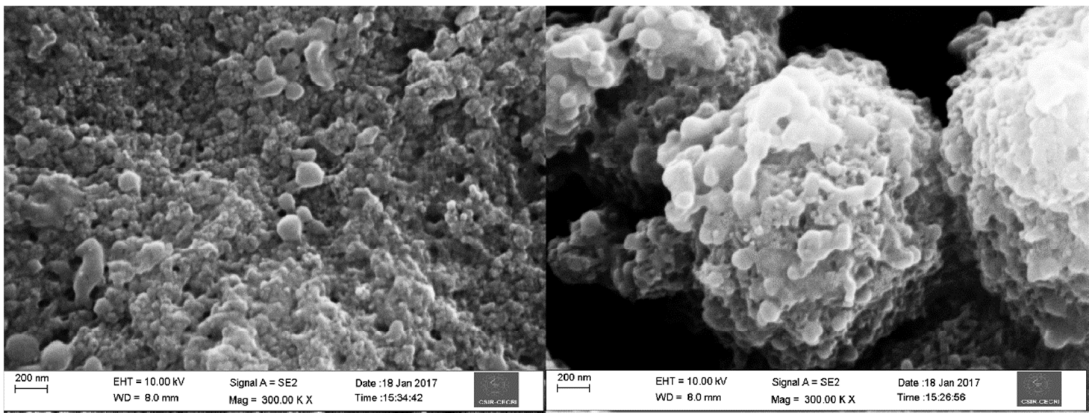

Figure S9. FE-SEM image of **EPOP**

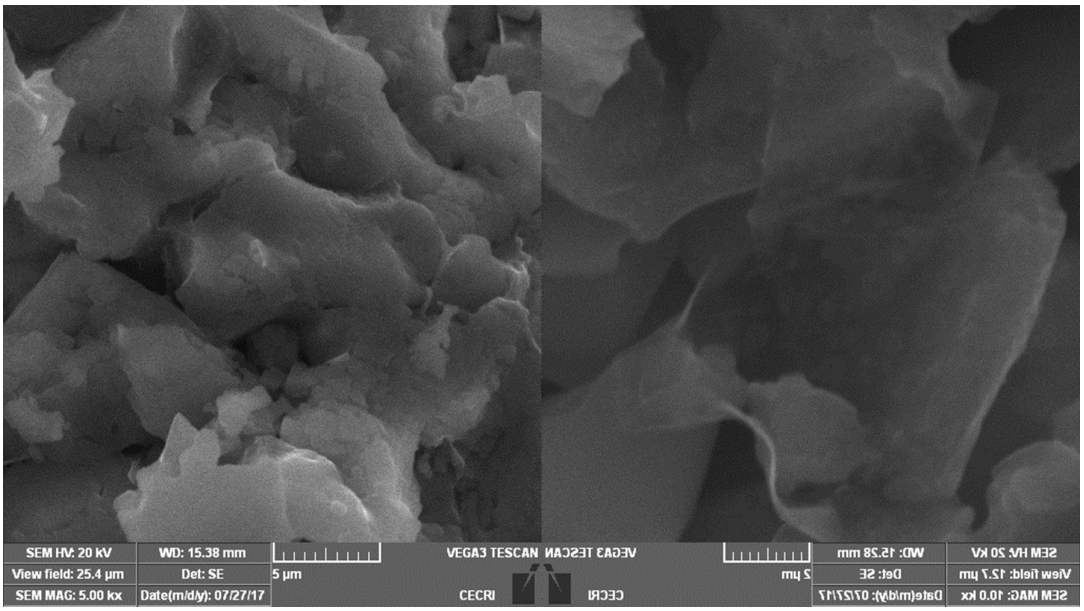

Figure S10. SEM image of **EPOP-600**

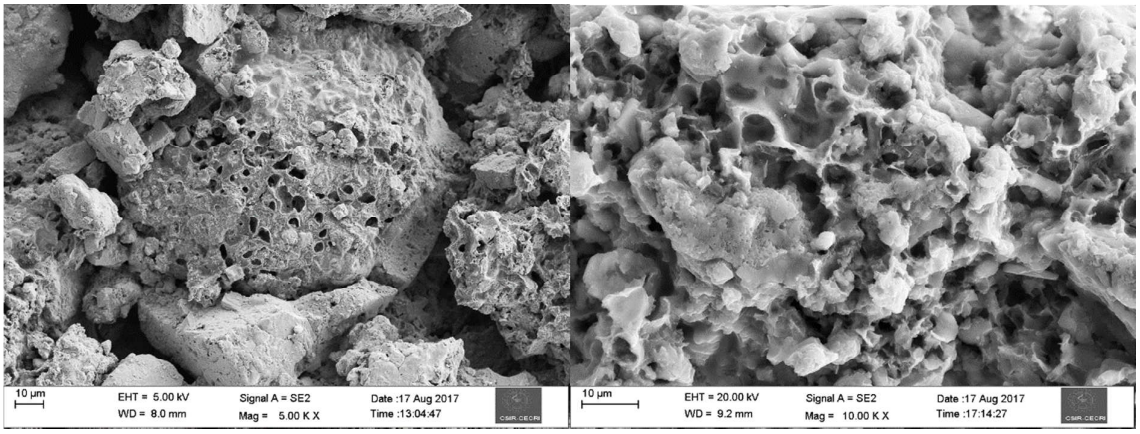

Figure S11. FE-SEM image of **EPOP-700**

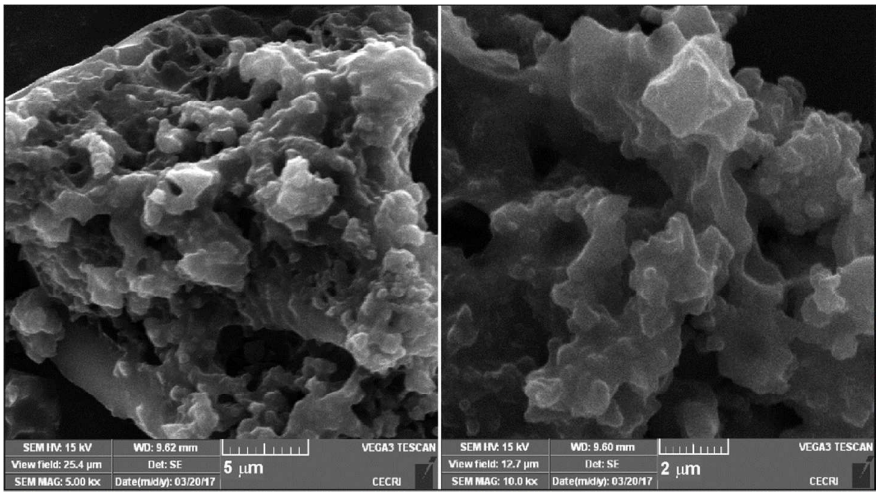

Figure S12. SEM image of **EPOP-800**

SI-Table 1. Carbon and Nitrogen content of the samples obtained from elemental analysis.

S.No	Catalyst	C%	N%	C/N ratio
1	EPOP	47.6	15.01	2.8
2	EPOP-600	58.97	15.06	3.5
3	EPOP-700	69.2	16.87	4.6
4	EPOP-800	63.1	16.4	4.2

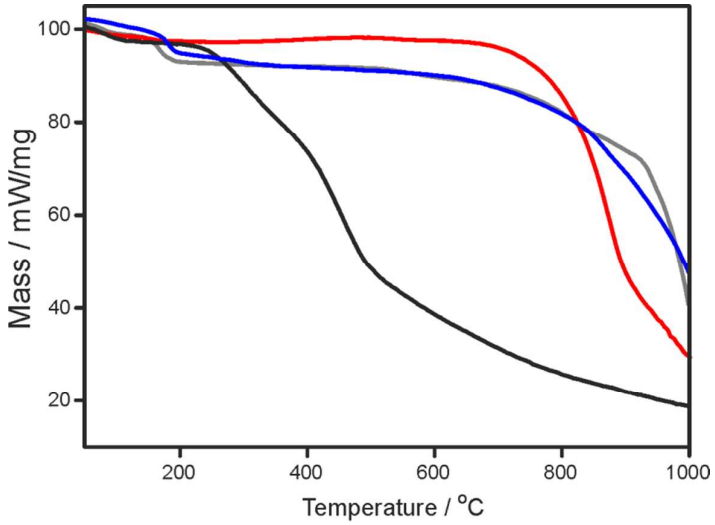

Figure S13. TGA profile of **EPOP** (black), **EPOP-600** (red), **EPOP-700** (blue) and **EPOP-800** (grey), corresponding weight losses were mentioned in %.

The thermal stability of the samples EPOP, EPOP-600, EPOP-700 and EPOP-800 were analysed by thermogravimetric analysis under nitrogen atmosphere (Figure S13). The thermal profile of EPOP indicated that there is a small weight loss of ~2.5 %, which is accompanied by the loss of water molecules. And subsequently, there was a gradual weight loss after 230 ºC indicating the loss of solvent molecules and decomposition of organic skeleton which lead to a 28% weight loss at 400 ºC. After 400 ºC there was a steep decrease in weight loss signifying the pyrolysis of organic moiety. Whereas the carbonised samples (EPOP-600ºC, EPOP-700 ºC, EPOP-800 ºC) exhibited 12 % weight loss around 350 ºCattributed to the loss of water molecules. The carbonized samples showed excellent thermal stability until 800 ºC.[1]

Active surface area Calculation

Using the same redox probe $K_3[Fe(CN)_6]$, the number of active sites in the surface of the electrode was calculated. The effective areas(A cm^{-2}) of all the carbon samples were estimated by using the Randles–Sevcik equation.

$$Ip = (2.69 \times 10^5)n^{2/3} A D^{1/2}\nu^{1/2} C$$

where D and C are the diffusion coefficient and concentration of the redox probe respectively, n is number of electron transfer and ν is scan rate (whole CV was run at 1 mV/s), the active area was calculated and given in table 2.

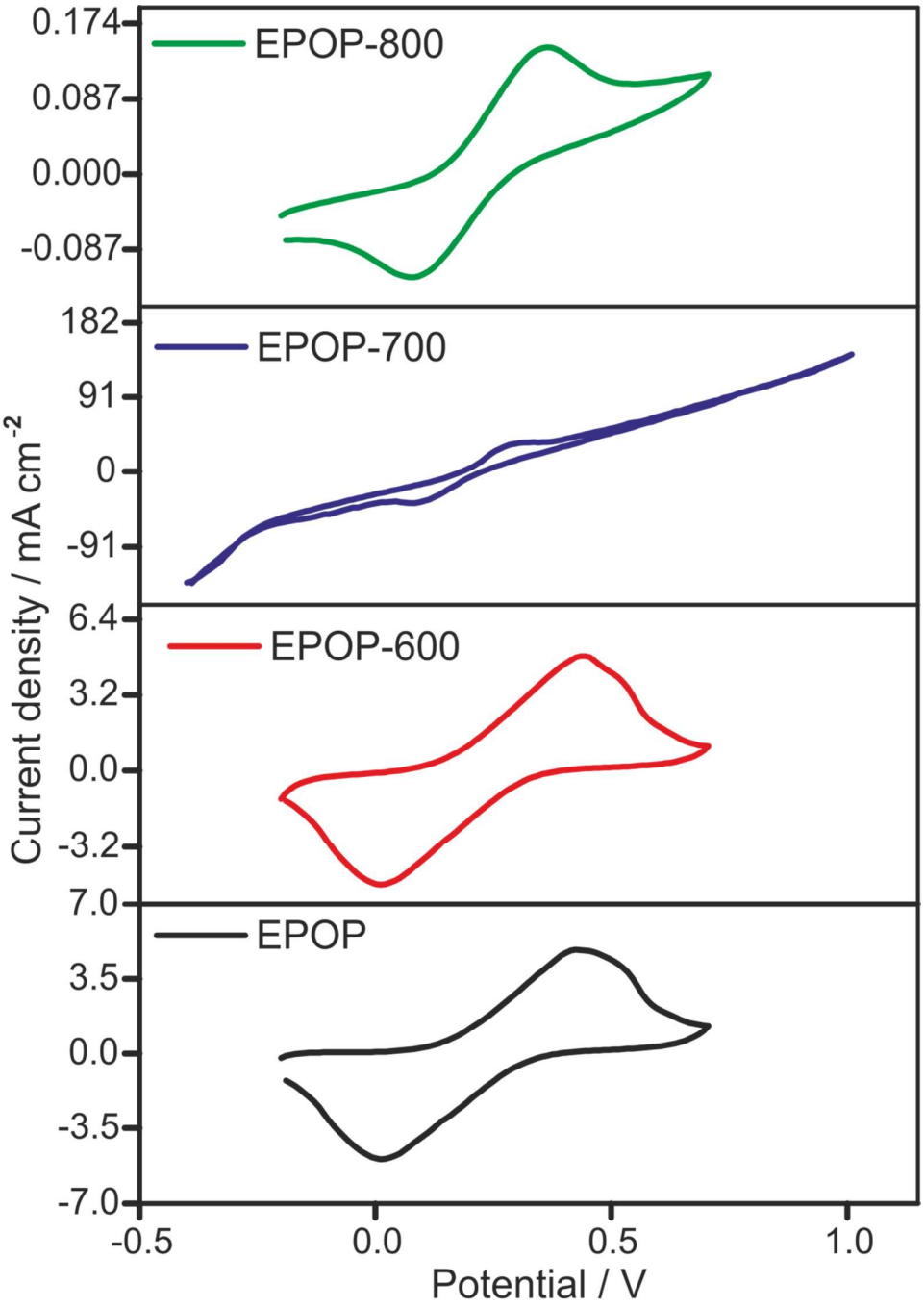

Figure S14. Ferro-Ferri response of modified electrode for active surface area calculations.

Figure S15. Image captured during **OER** (**EPOP-700** modified electrode**)**

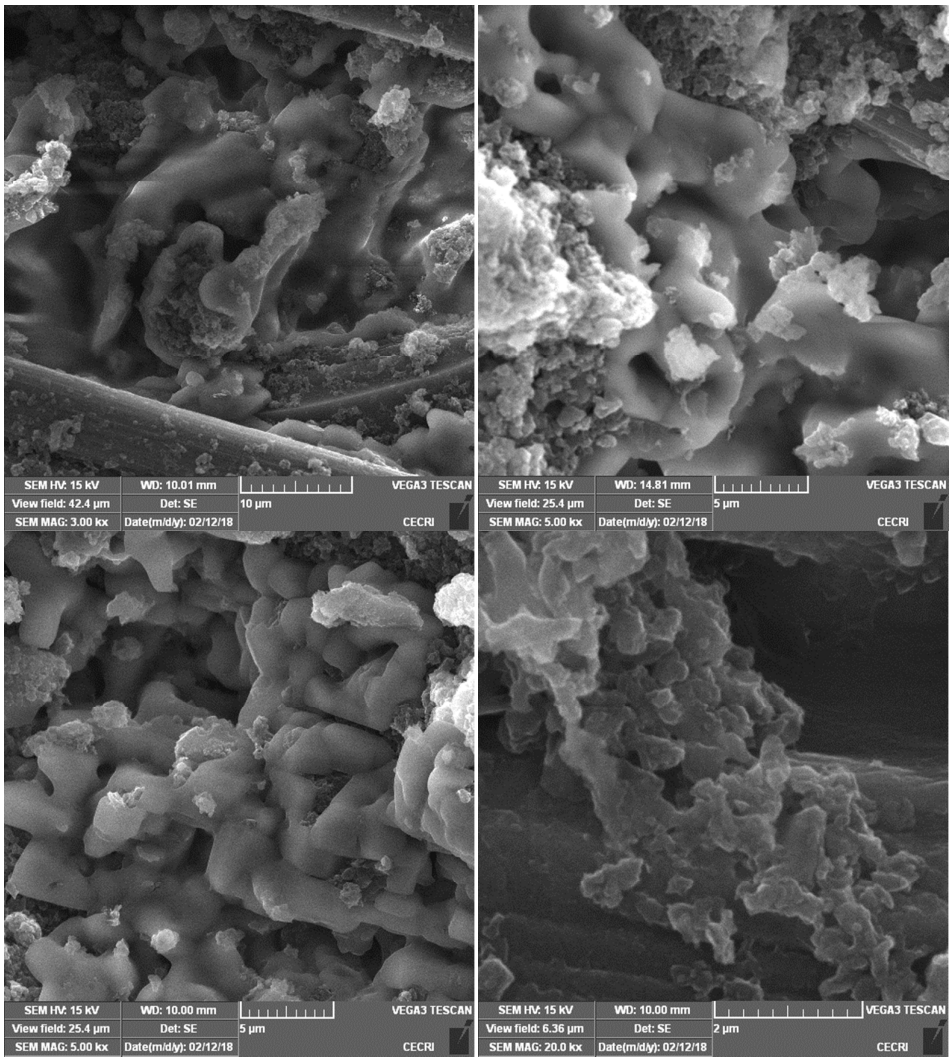

Figure S16. SEM image of the modified electrode with **EPOP-700** sample after OER measurements.

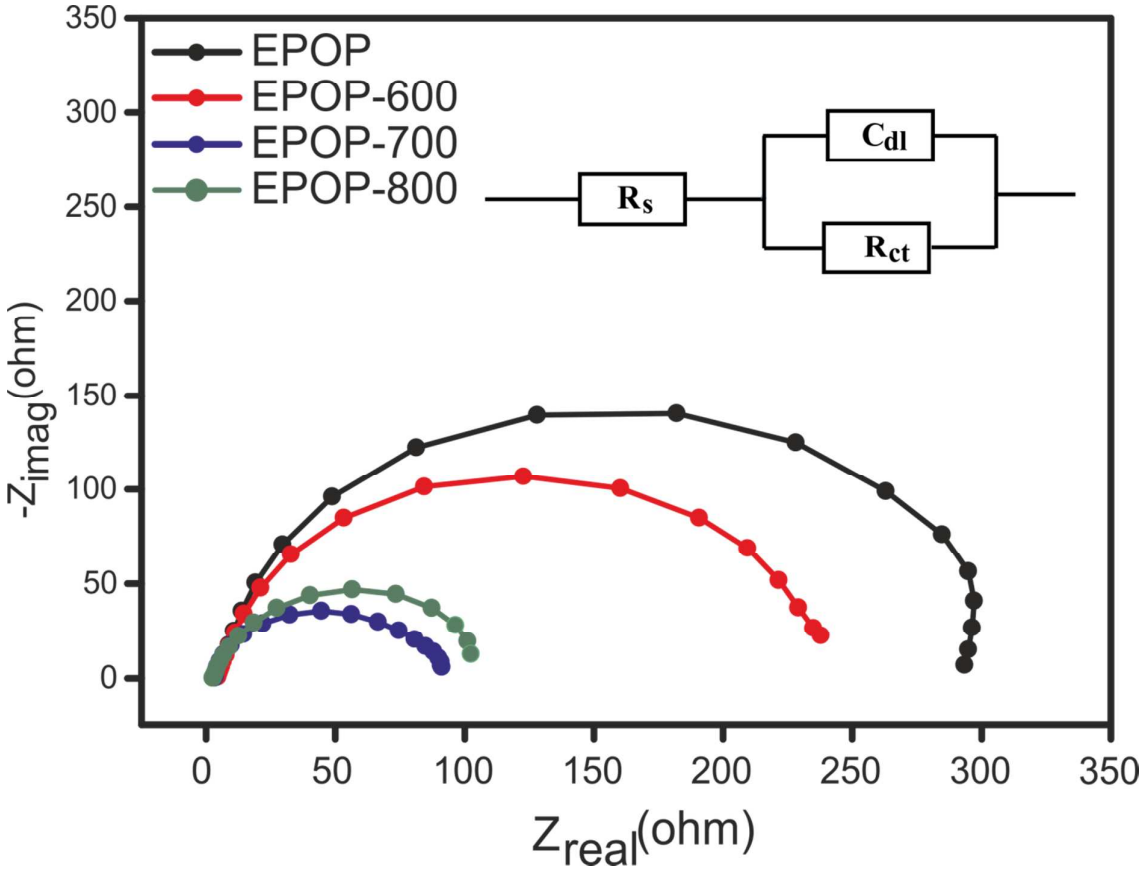

Figure S17. EIS spectra of **EPOP**, **EPOP-600**, **EPOP-700** and **EPOP-800**.

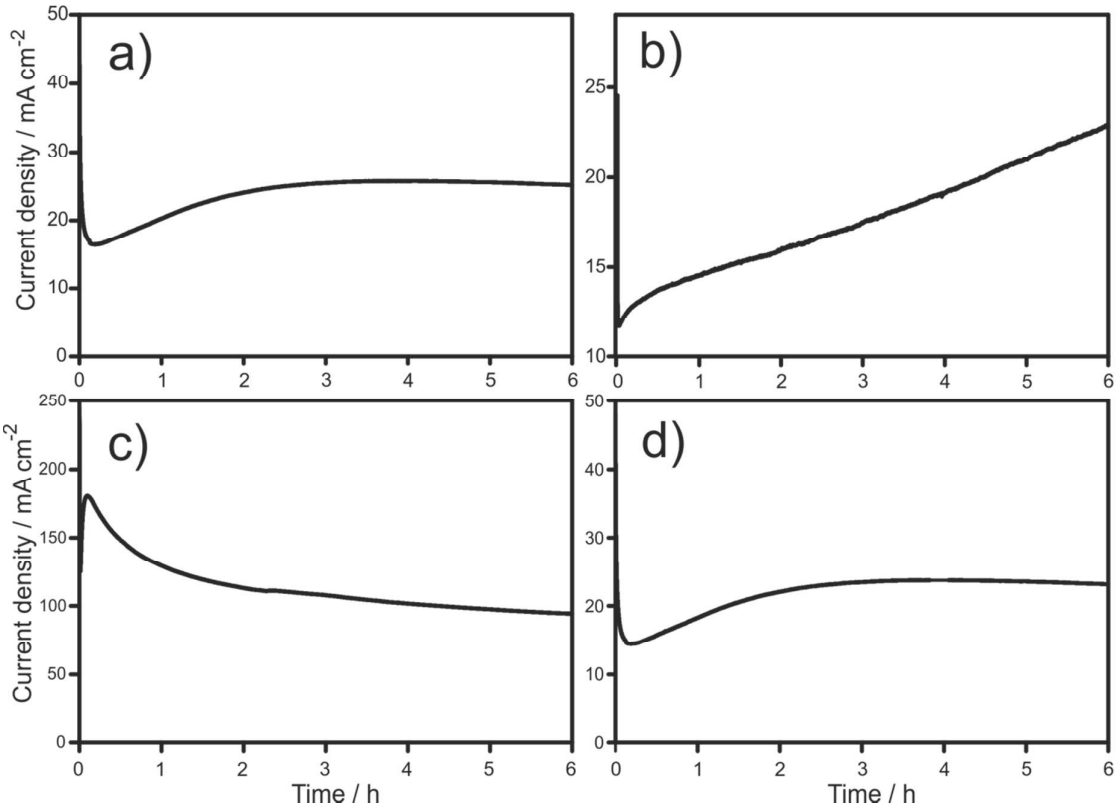

Figure S18. Chronoamperometry curve depicting the **s**tability of a) EPOP, b) EPOP-600, c) EPOP-700 and d) EPOP-800 samples for the duration of 6 h**.**

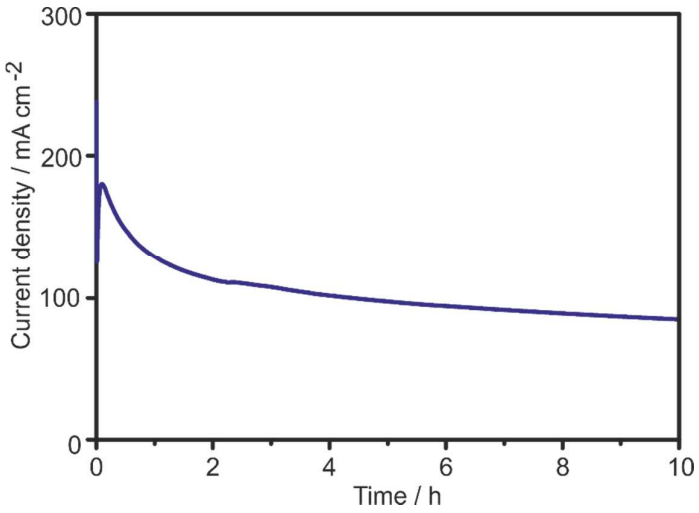

Figure S19. Chronoamperometry curve depicting the **s**tability of **EPOP-700** sample for the duration of 10 h**.**

XPS analysis

We propose that the better activity can be attributed to the presence of nitrogen atom and this will impart a positive charge on the carbon due to their prevailing electronegativity values. (i.e., electronegativity of C and N is 2.55 and 3.04 respectively). To substantiate our idea, we have carried out XPS analysis for EPOP-700 and included in the revised manuscript. From the survey spectrum of EPOP-700 sample, we found out the presence of C 1s, N 1s, O1s respectively The high-resolution N1s spectra are curve fitted into two individual peaks (Fig. b) pyridinic N (398.2 eV), pyrrolic N (402.3 eV).The presence of pyridinic nitrogen in the EPOP-700 sample clearly explains the presence of nitrogen atom with a negative charge bonded to an adjacent carbon (Atomic scale characterization of nitrogen-doped graphite: Effects of the dopant nitrogen on the electronic structure of the surrounding carbon atoms). From the C1s spectra shows three major peaks at 284.9eV, 286.3eV and 290.8eV respectively. The peak at 284.9 eV corresponds to the sp2 -hybridized graphitic carbon, the peaks at 286.3 and 290.8 eV are attributed for C-N bond and C=O bond. From the O1s shows two peaks at 532.7 and 536.9eV, which may attributed to the surface C-O and hydroxyl groups. From the XPS analysis, the presence of C-N bond is evident with a negatively charged N atom. Based on this, we have proposed the adsorption of hydroxide ions to the carbon adjacent to nitrogen. Also similar kind of observation is also made in the literature.

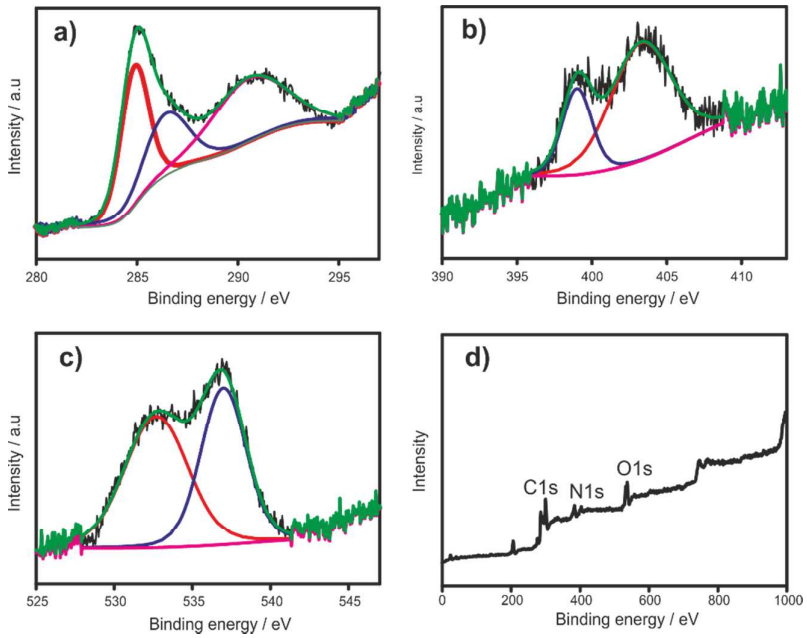

Figure S20. XPS analysis of **EPOP-700** sample; core level spectra of a) Carbon, b) Nitrogen, c) Oxygen and d) survey spectra.

Effect of pH on OER activity

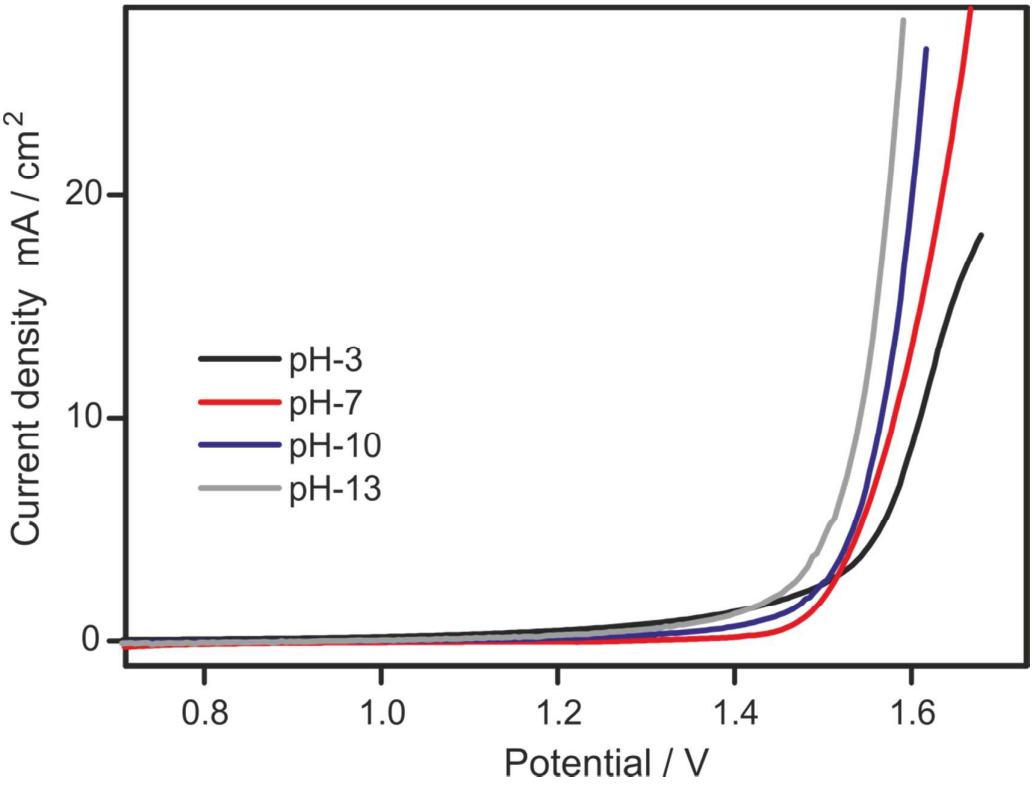

Figure S21. Effect of pH on OER activity (EPOP-700)

pH	Onset (10 mA)	Overpotential (mV)
3	1.61	380
7	1.579	349
10	1.56	335
13	1.541	311

SI-Table 2. Comparison of OER onset potential and current density of carbon materials

S.No	Materials	Onset potential (V) *vs.* RHE	Current Density (mA cm^{-2})	Ref.
1	Graphitic Carbon, Nitride Nanosheet Carbon Nanotube	g-C_3N_4 NS–CNT=1.53	10	[2]
2	Nitrogen and Phosphorus Dual-Doped Graphene/Carbon Nanosheets	N,P-GCNS = 1.32	70.75	[3]
		N,P-CNS = 1.41	15.57	
		NCNP = 1.78	0.78	
	Nitrogen-doped graphene	1.61	10	
3	Pyrolyzed COF(Like graphene)	1.58	0.18	[4]
4	Graphene	1.75	10	[5]
5	Nitrogen-Doped carbon nanotube	0.8 *vs*. SCE	10	[6]
6	Graphene	1.54 V	20	[7]
7	Nitrogen-doped carbon nanomaterials	N/C=1.52±0.02	10	[8]
8	Carbon nanotube	O-CNT=1.55 R-CNT=1.64	10	[9]
0	Nitrogen-Doped Graphene/Carbon Nanotube	1.63	10	[10]
10	N-doped graphene	1.5 - 1.8	10	[11]
11	Nitrogen doped graphene	1.8	1	[12]
12	Sulfur-Doped Carbon Nanotube–GrapheneNanolobes	1.63	10	[13]

13	**EPOP**	1.673	53	This work
	EPOP-600	1.70	22	
	EPOP-700	1.527	322	
	EPOP-800	1.65	37	

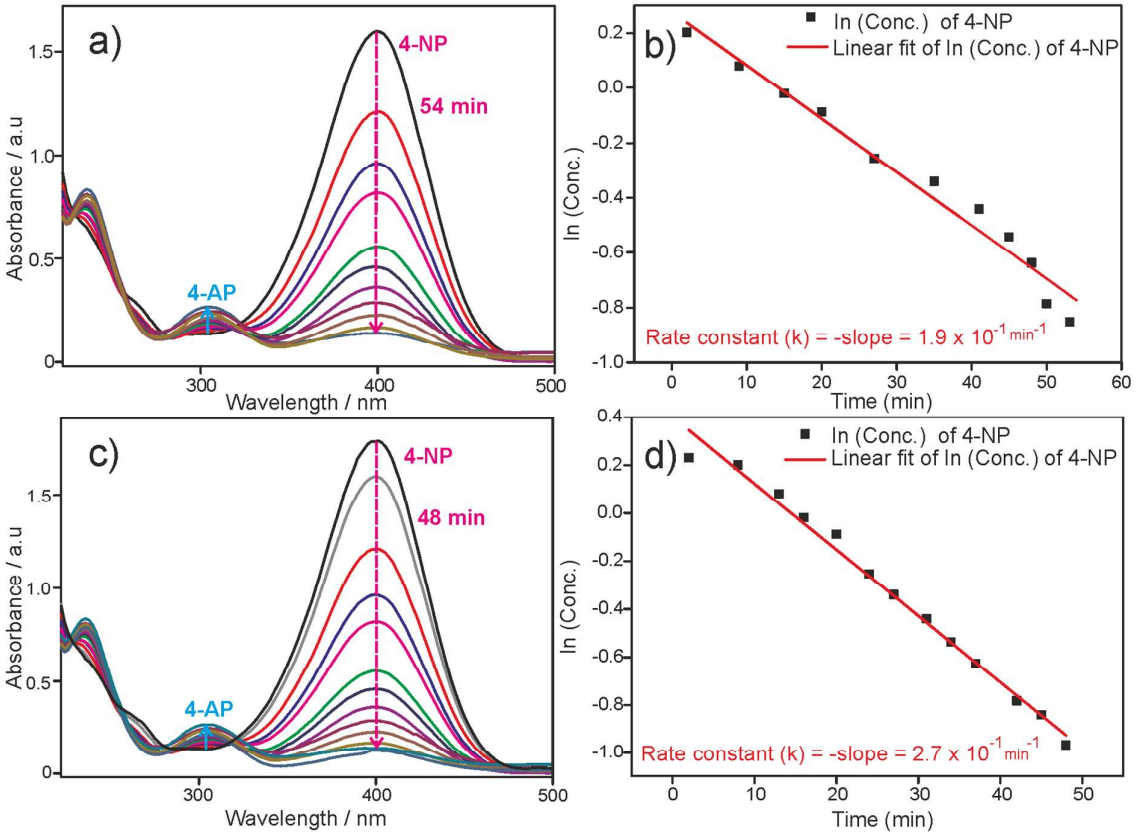

Figure S21. UV-Vis absorption spectra for the catalytic reduction of 4-nitrophenol by $NaBH_4$ over a) EPOP, c) EPOP-600, and the corresponding linear fit is shown in b) EPOP, and d) EPOP-600.

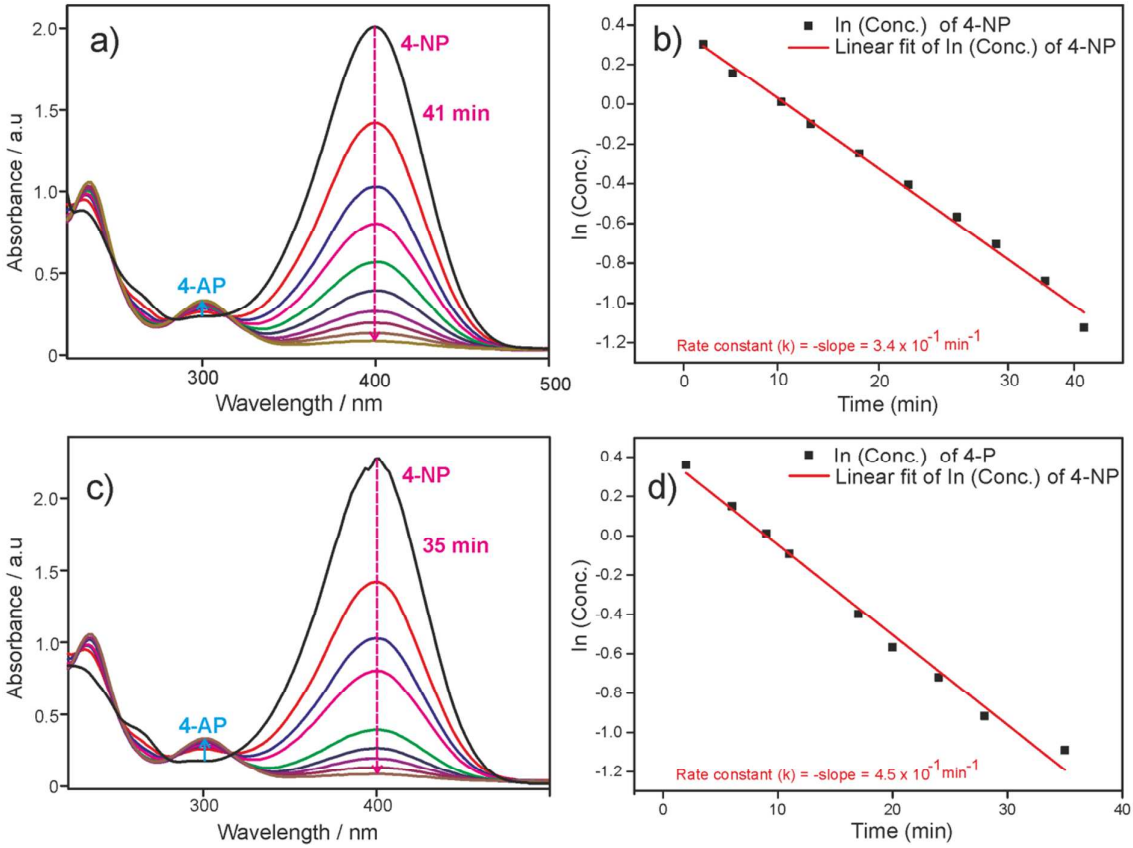

Figure S22. UV-Vis absorption spectrum for the catalytic reduction of 4-nitrophenol by $NaBH_4$ over a) EPOP-700, c) EPOP-800, and the corresponding linear fit is shown in b) EPOP-700, and d) EPOP-800.

SI-Table-3. Catalysts and their corresponding rate constants obtained from UV-Vis measurements

S.No.	Catalyst	Rate Constant (10^{-1} min^{-1})
1	EPOP	1.9
2	EPOP-600	2.7
3	EPOP-700	3.4
4	EPOP-800	4.5

Supporting References

1. Tao, L.-M.; Niu, F.; Zhang, D.; Wang, T.-M.; Wang, Q.-H., Amorphous covalent triazine frameworks for high performance room temperature ammonia gas sensing. *New J. Chem.* **2014,***38* (7), 2774-2777.

2. Ma, T. Y.; Dai, S.; Jaroniec, M.; Qiao, S. Z., Graphitic Carbon Nitride Nanosheet–Carbon Nanotube Three-Dimensional Porous Composites as High-Performance Oxygen Evolution Electrocatalysts. *Angew. Chem. Int. Ed.* **2014,***53* (28), 7281-7285.

3. Li, R.; Wei, Z.; Gou, X., Nitrogen and Phosphorus Dual-Doped Graphene/Carbon Nanosheets as Bifunctional Electrocatalysts for Oxygen Reduction and Evolution. *ACS Catal.* **2015,***5* (7), 4133-4142.

4. Qian, Y.; Hu, Z.; Ge, X.; Yang, S.; Peng, Y.; Kang, Z.; Liu, Z.; Lee, J. Y.; Zhao, D., A metal-free ORR/OER bifunctional electrocatalyst derived from metal-organic frameworks for rechargeable Zn-Air batteries. *Carbon* **2017,***111*, 641-650.

5. Xiao, Z.; Huang, X.; Xu, L.; Yan, D.; Huo, J.; Wang, S., Edge-selectively phosphorus-doped few-layer graphene as an efficient metal-free electrocatalyst for the oxygen evolution reaction. *Chem. Commun.* **2016,***52* (88), 13008-13011.

6. Tian, G.-L.; Zhang, Q.; Zhang, B.; Jin, Y.-G.; Huang, J.-Q.; Su, D. S.; Wei, F., Toward Full Exposure of "Active Sites": Nanocarbon Electrocatalyst with Surface Enriched Nitrogen for Superior Oxygen Reduction and Evolution Reactivity. *Adv. Funct. Mater.* **2014,***24* (38), 5956-5961.

7. Liang, Y.; Li, Y.; Wang, H.; Zhou, J.; Wang, J.; Regier, T.; Dai, H., Co3O4 nanocrystals on graphene as a synergistic catalyst for oxygen reduction reaction. *Nat. Mater.* **2011,***10* (10), 780-786.

8. Zhao, Y.; Nakamura, R.; Kamiya, K.; Nakanishi, S.; Hashimoto, K., Nitrogen-doped carbon nanomaterials as non-metal electrocatalysts for water oxidation. *Nat. Commun.* **2013,***4*, 2390.

9. Li, L.; Yang, H.; Miao, J.; Zhang, L.; Wang, H.-Y.; Zeng, Z.; Huang, W.; Dong, X.; Liu, B., Unraveling Oxygen Evolution Reaction on Carbon-Based Electrocatalysts: Effect of Oxygen Doping on Adsorption of Oxygenated Intermediates. *ACS Energy Lett.* **2017,***2* (2), 294-300.

10. Tian, G.-L.; Zhao, M.-Q.; Yu, D.; Kong, X.-Y.; Huang, J.-Q.; Zhang, Q.; Wei, F., Nitrogen-Doped Graphene/Carbon Nanotube Hybrids: In Situ Formation on Bifunctional

Catalysts and Their Superior Electrocatalytic Activity for Oxygen Evolution/Reduction Reaction. *Small* **2014,***10* (11), 2251-2259.

11. Yang, H. B.; Miao, J.; Hung, S.-F.; Chen, J.; Tao, H. B.; Wang, X.; Zhang, L.; Chen, R.; Gao, J.; Chen, H. M.; Dai, L.; Liu, B., Identification of catalytic sites for oxygen reduction and oxygen evolution in N-doped graphene materials: Development of highly efficient metal-free bifunctional electrocatalyst. *Sci. Adv.* **2016,***2* (4).

12. Wang, J.; Lin, W.-F.; Shi, Y.; Wang, H.-S.; Rong, L.-Q.; Xia, X.-H., A simple way to fine tune the redox potentials of cobalt ions encapsulated in nitrogen doped graphene molecular catalysts for the oxygen evolution reaction. *Chem. Commun.* **2016,***52* (91), 13409-13412.

13. El-Sawy, A. M.; Mosa, I. M.; Su, D.; Guild, C. J.; Khalid, S.; Joesten, R.; Rusling, J. F.; Suib, S. L., Controlling the Active Sites of Sulfur-Doped Carbon Nanotube–Graphene Nanolobes for Highly Efficient Oxygen Evolution and Reduction Catalysis. *Adv. Energy Mater.* **2016,***6* (5), 1501966.